
Article:

Capel Berdiell, I, Warriner, SL and Halcrow, MA (2018) Silver(i) complexes of bis- and tris-(pyrazolyl)azine derivatives - dimers, coordination polymers and a pentametallic assembly. Dalton Transactions, 47 (15). pp. 5269-5278. ISSN: 1477-9226

https://doi.org/10.1039/c8dt00640g

Silver(I) Complexes of *Bis*- and *Tris*-(pyrazolyl)azine Derivatives – Dimers, Coordination Polymers and a Pentametallic Assembly†‡

Izar Capel Berdiell, Stuart L. Warriner and Malcolm A. Halcrow*

Silver(I) complexes of 2,4,6-tri(pyrazol-1-yl)pyridine (tpp), 2,4,6-tri(pyrazol-1-yl)pyrimidine (tpym), 2,4,6-tri(pyrazol-1-yl)-1,3,5-triazine (tpt) and 2,4-di(pyrazol-1-yl)-1,3,5-triazine (bpt) are reported. Dinuclear $[Ag_2(\mu\text{-tpp})_2(MeCN)_2][BF_4]_2{\cdot}2MeCN$ and $[Ag_2(\mu\text{-tpym})_2(MeCN)_2][BF_4]_2$ are formed from approximately planar $[AgL(NCMe)]^+$ (L = tpp or bpym) centres, which dimerise *via* apical interactions to the pendant pyrazolyl donor on each ligand. Two polymeric solvatomorph phases $[Ag_2(\mu\text{-tpp})_2][BF_4]_2{\cdot}n\text{MeNO}_2$ were obtained by crystallising $AgBF_4$ and tpp from nitromethane solution. One is composed of the same dimeric $[Ag_2(\mu\text{-tpp})_2]^{2+}$ motif as the MeCN solvates, but with semibridging pyrazolyl substitutents replacing the solvent ligands. The other form has helicate $[Ag_2(\mu\text{-tpp})_2]^{2+}$ dimers linked into chains by unsupported Ag...Ag interactions. In contrast, $[Ag_5(\mu_3\text{-tpym})_4][BF_4]_5{\cdot}2MeNO_2$ contains discrete pentametallic assemblies, of a flattened $[Ag_4(\mu\text{-tpym})_4]^{4+}$ molecular square centred by the fifth silver ion. Three helical or linear 1D coordination polymer topologies are described for $[Ag(\mu\text{-tpt})]X$ (X^- = BF_4^- or ClO_4^-), where ditopic tpt ligands bind one silver ion in a [2+1] geometry and the other in bidentate, [1+1] or monodentate fashion. Finally, $[Ag(bpt)]BF_4$ is a polymer of square planar silver ions linked by *bis*-bidentate bpt ligands. Most of the tpt and bpt structures include short anion...π contacts to the ligand triazinyl rings. Electrospray mass spectra confirm the oligomeric nature of the Ag/tpym and tpt complexes in $MeNO_2$ solution.

Introduction

Complexation of silver(I) salts with 2,2':6',2''-terpyridine (terpy) and its derivatives yields a variety of assembly structures, which are mostly based on two recurring motifs. First, are approximately planar [Ag(terpy)X] or $[Ag(terpy)L]^+$ centres (X^- = anion, L = solvent or another monodentate ligand),[1-7] which may aggregate into dimers or coordination polymers if L is a bridging ligand,[8-15] or *via* intermolecular Ag...Ag argentophilic interactions in the crystalline state.[2,3] Alternatively, $[Ag_n(terpy)_m]^{n+}$ helicate structures are also well-known, usually in dimeric complexes (n = m = 2)[4-6,15-18] although larger molecular[1,6] or polymeric[6] helicate assemblies of this type are also known. Other "terpyridine analogue" *tris*-heterocycles also mostly yield square planar dimers[19] or helicate assemblies[20-26] when complexed to silver(I). However examples of circular helicates,[22] molecular squares[27] and rare homoleptic octahedral silver(I) complexes[23] have also been reported with such ligands.

Our interest in the coordination chemistry of 2,6-di-(pyrazolyl)pyridine (bpp) and its derivatives has given us access to a number of di- and tri-(pyrazolyl)azine chelates.[28,29] Few coinage metal complexes with such ligands have been reported up to now, most of which are $[Ag_2(\mu\text{-bpp})_2]^{2+}$-type helicate dimers[21] although one polymeric helicate structure of this type is also known.[25] We reasoned that a third pyrazolyl ring at the periphery of the bpp ligand framework might link $[Ag_n(bpp)_m]^{n+}$-type fragments into higher order assemblies. We therefore report a crystallographic study of silver(I) complexes of 2,4,6-tri(pyrazol-1-yl)pyridine (tpp), and two other *tris*-pyrazolyl-azines 2,4,6-tri(pyrazol-1-yl)pyrimidine (tpym) and 2,4,6-tri(pyrazol-1-yl)-1,3,5-triazine (tpt; Scheme 1). The synthesis and silver complex of the new ligand 2,4-di(pyrazol-1-yl)-6*H*-1,3,5-triazine (bpt) are also briefly described.

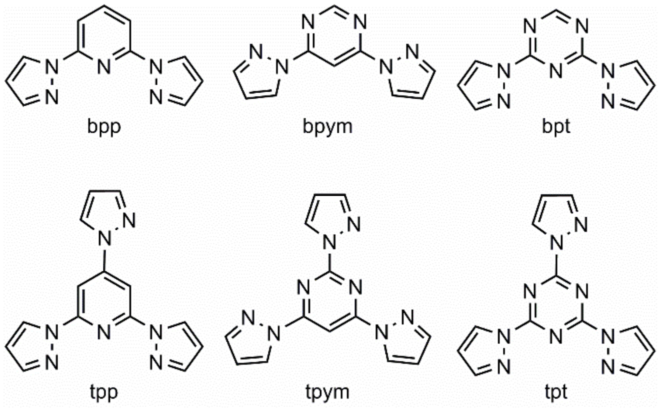

Scheme 1 Ligands referred to in this work.

School of Chemistry, University of Leeds, Leeds, UK LS2 9JT. Fax: (+44) 113 343 6565. E-mail: m.a.halcrow@leeds.ac.uk

†Electronic Supplementary Information (ESI) available: additional crystallographic Figures and Tables; X-ray powder diffraction data; and, NMR and mass spectra. CCDC-1569518-1569527 and 1815532. See DOI: 10.1039/x0xx00000x

‡ Data supporting this study are available at http://doi.org/10.5518/346.

Results and Discussion

2,4-Di-(pyrazol-1-yl)-6*H*-1,3,5-triazine (bpt, Scheme 1) was obtained in moderate yield, by reaction of 2,4-dichloro-6*H*-1,3,5-triazine with 2 equiv of deprotonated pyrazole in THF. The other ligands tpp,[29] tpym[30] and tpt[31] were prepared by the literature procedures. All the complexes were prepared by co-crystallising 1:1 mole ratios of the appropriate ligand and silver salt, in the solvents stated below, using diethyl ether vapour as anti-solvent. The Ag–N distances in the structures range from 2.15-2.96 Å, with bonds to pyrazolyl groups mostly being shorter than to the azinyl N-donors (ESI†). Although the boundary is arbitrary, Ag–N bonds of <2.65 Å are considered as full bonds in the following discussions, and Ag–N/O/F distances >2.65 Å as weaker secondary interactions.

Co-crystallisation of a 1:1 ratio of $AgBF_4$ and tpp from MeCN yields $[Ag_2(\mu\text{-tpp})_2(NCMe)_2][BF_4]_2\cdot 2MeCN$ (**1**·2MeCN; monoclinic, $P2_1/c$), featuring a centrosymmetric $[Ag_2(\mu\text{-tpp})_2(NCMe)_2]^{2+}$ dication. The unique silver ion has a distorted square pyramidal coordination geometry ($\tau = 0.38$,[32] ESI†) with basal tridentate tpp ligands, and the bridging pyrazolyl donor $N(19^i)$ in the apical position (Fig. 1). The tridentate cores of the ligands are co-parallel with a least squares interplanar distance of 3.30(3) Å, implying a significant $\pi ... \pi$ interaction between them. The Ag...Ag distance within the dimer is 7.2461(7) Å. The same dimeric motif also occurs in several silver complexes, of terpy derivatives bearing pendant donor groups.[6,8-11] The cations in **1**·2MeCN form canted stacks parallel to the unit cell *b* direction, *via* an intermolecular $\pi ... \pi$ interaction between their (almost) planar tridentate ligand domains.

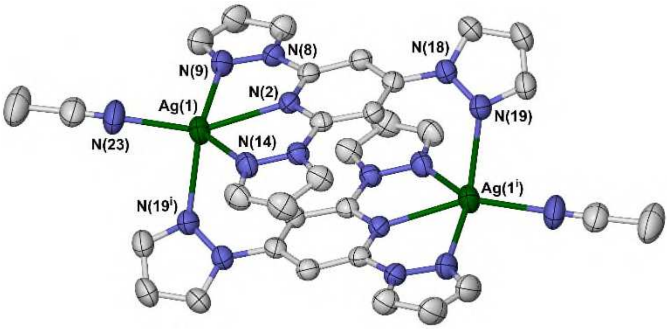

Figure 1 The centrosymmetric $[Ag_2(\mu\text{-tpp})_2(NCMe)_2]^{2+}$ cation in **1**·2MeCN. Atomic displacement ellipsoids are at the 50 % probability level, and H atoms are omitted for clarity. The $[Ag_2(\mu\text{-tpym})_2(NCMe)_2]^{2+}$ complex in **3** is shown in the ESI†. Symmetry code: (i) 1–*x*, 1–*y*, 1–*z*. Colour code C, white; H, grey; Ag, green; N, blue.

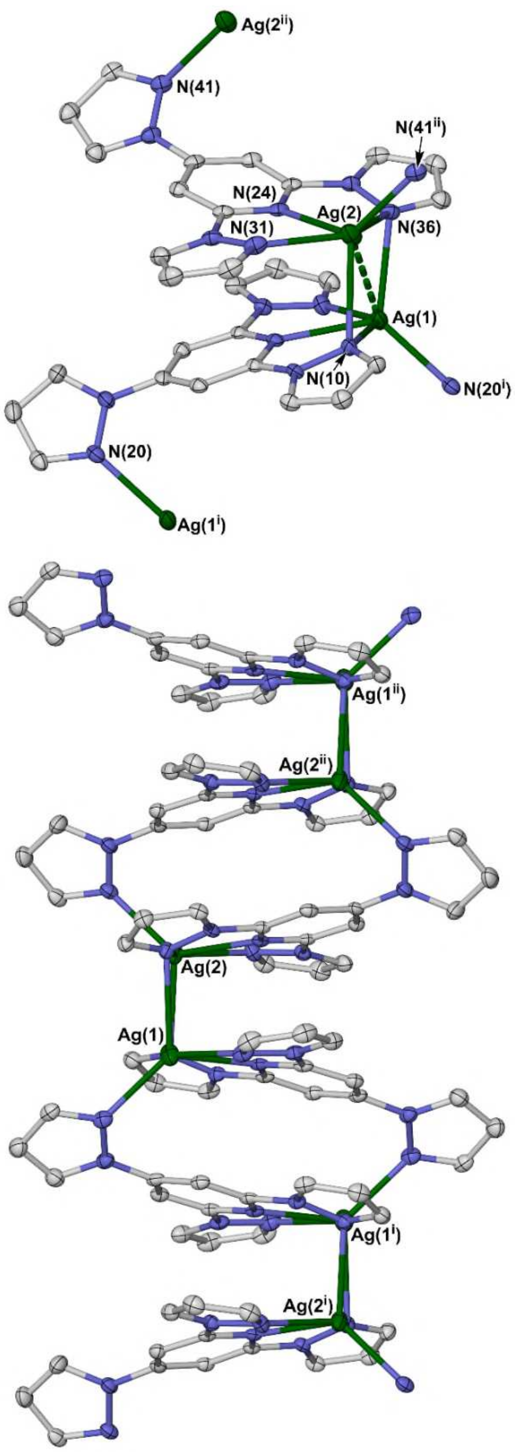

Figure 2 Top: the coordination polymer asymmetric unit in α-**2**·$MeNO_2$. Bottom: the 1D polymer structure, showing its resemblance to the $[Ag_2(\mu\text{-tpp})_2(NCMe)_2]^{2+}$ dimer (Fig. 1). The view is along the $(11\bar{1})$ crystallographic vector. Other details as for Fig. 1. Symmetry codes: (i) 1–*x*, 1–*y*, 1–*z*; (ii) 1–*x*, 1–*y*, –*z*.

Reaction of the same metal/ligand combination in $MeNO_2$ instead yielded a mixture of cubic and prismatic morphologies, which respectively proved to be the pseudo-polymorphs $[Ag_2(\mu_3\text{-tpp})_2][BF_4]_2\cdot MeNO_2$ (α-**2**·$MeNO_2$) and $[Ag_2(\mu\text{-tpp})_2][BF_4]_2\cdot y MeNO_2$ (β-**2**·$y MeNO_2$, $y \approx 0.3$). The majority form is α-**2**·$MeNO_2$ (triclinic, $P\bar{1}$), which was the only one to be isolated in pure form by powder diffraction (ESI †). The compound is a 1D coordination polymer formed from $[Ag_2(\mu\text{-tpp})_2]^{2+}$ moieties that clearly resemble the dimeric molecule in **1** (Fig. 2). The asymmetric unit contains two half-dimers, each spanning a crystallographic centre of symmetry. However, in place of the coordinating solvent, the fifth coordination site on each silver ion is occupied by a symmetrically bridging pyrazolyl N-donor from the neighbouring dimer (Fig. 2). The bridging Ag–N(10) and Ag–N(36) distances lie between 2.520(2)-2.636(2) Å, which is 0.15-0.20 Å longer than the other Ag–N bonds in the molecule (ESI†). This $\kappa^1,\kappa^1:\mu$ coordination mode is unusual in pyrazole complexes,[33,34] with most examples being found in poly-pyrazolylborate chemistry.[33] The two unique silver ions have more regular square pyramidal geometries than in **1** (τ = 0.06[32]), with the bridging pyrazolyl groups occupying basal and apical coordination sites. The bridging interactions associate the complex into chains-of-dimers, running parallel to the unit cell *c* direction. The Ag...Ag distances within the chains are 6.8167(7)-6.8762(7) Å (intradimer) and 3.2497(4) Å (interdimer).

The asymmetric unit of the other solvatomorph β-**2**·*y*MeNO$_2$ ($y \approx 0.3$; monoclinic, $P2_1/c$) contains four Ag/tpp moieties, which are organised into a pair of $[\mathrm{Ag}_2(\mu\text{-tpp})_2]^{2+}$ dimers with a helicate topology (Fig. 3). The tpp ligands in this case are only coordinated through the tridentate metal-binding domain, with the pendant 4-pyrazolyl groups projecting from the periphery of the molecules. The silver ions are coordinated near-linearly to the one pyrazolyl group from each ligand in their dimer [N{pyrazolyl}–Ag–N{pyrazolyl} = 169.90(19)-178.51(18) Å], with differing patterns of weaker interactions to the central pyridyl donors. In dimer Ag(1)/Ag(2), the tpp pyridyl groups N(5) and N(26) are clearly semi-bridging, with the Ag...N{pyridyl} bond lengths to Ag(1) being 0.212(7)-0.240(7) Å longer than to Ag(2). In contrast, in dimer Ag(3)/Ag(4) the pyridyl donors N(47) and N(68) are bound more symmetrically, with the Ag...N{pyridyl} bond lengths to Ag(4) being only 0.075(7)-0.097(7) Å longer than to Ag(3). The silver ions in each dimer are separated by 2.9089(6)-2.9108(6) Å, while the dimers are in turn linked into chains by unsupported Ag...Ag interactions of 3.0415(6)-3.0660(6) Å. The helical chains are co-aligned parallel to the unit cell b direction, with stripes of Λ and Δ helical chains alternating along *a* in the centrosymmetric crystal (ESI†).

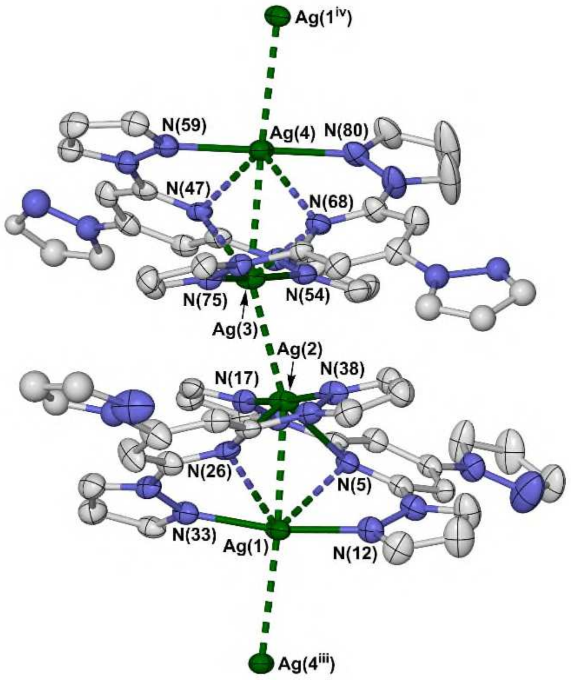

Figure 3 The coordination polymer asymmetric unit in β-**2**·*y*MeNO$_2$. Only one orientation of the three disordered, non-coordinated pyrazolyl groups is shown. Other details as for Fig. 1. Symmetry codes: (iii) *x*, –1+*y*, *z*; (iv) *x*, 1+*y*, *z*.

The dimeric helicate motif is well-known in coinage metal complexes of *tris*-heterocycle ligands,[4-6,15-18,20-24] including derivatives of bpp (Scheme 1).[21] Rare examples of such dimeric helicates associating into higher order molecular assemblies through unsupported dispersion interactions are known.[17,18] However, the "unsupported chain of helicate dimers" motif in β-**2**·*y*MeNO$_2$ is unique to our knowledge. This is a topological isomer of the continuous spiral structure adopted by other helicate polymers of this type, where each pair of silver ions is bridged by one tridentate ligand.[6,25,26]

MeCN solutions of 1:1 AgBF$_4$ and tpym yielded crystalline $[\mathrm{Ag}_2(\mathrm{tpym})_2(\mathrm{NCMe})_2][\mathrm{BF}_4]_2$ (**3**; monoclinic, $P2_1$), featuring a $[\mathrm{Ag}_2(\mu\text{-tpym})_2(\mathrm{NCMe})_2]^{2+}$ dication with the same connectivity as **1** (Fig. 1 and ESI†). Although their unit cell dimensions are similar, the complex molecule in **3** does not have the crystallographic inversion symmetry present in **1**·2MeCN. This is reflected in the dispositions of the two tpym ligands in the molecule, whose monodentate pyrazolyl groups are oriented *cisoid* to each other. In contrast, the tpp ligands in **1**·2MeCN have their monodentate pyrazolyl groups in a *transoid* orientation (ESI†). In other respects, the metric parameters and crystal packing in these two compounds show only small differences.

In contrast to the Ag/tpp complexes, however, complexation of AgBF$_4$ and tpym from MeNO$_2$ yields a discrete molecular assembly $[\mathrm{Ag}_5(\mu_3\text{-tpym})_4][\mathrm{BF}_4]_5\cdot 2\mathrm{MeNO}_2$ (**4**·2MeNO$_2$; monoclinic, $C2/c$). Analysis of this structure is complicated by channels running parallel to the unit cell *b* direction, representing 26 % of the total unit cell volume. The channels have a dumbbell shape, with a width of 11.2 Å and height varying between 0.2-2.7 Å (ESI†). The disordered pore contents include three of the five anions expected for charge balance, and the solvent content of the crystal which was estimated from a *SQUEEZE* analysis.[35]

The complex molecule in **4** has C_2 symmetry with Ag(1), Ag(2) and Ag(3) lying on the crystallographic C_2 axis (Fig. 4). The cluster is a rhombus of Ag(2), Ag(3), Ag(4) and Ag(4^{xviii}) [symmetry code: (xviii) 1–*x*, *y*, $^3/_2$–*z*], linked by four tpym ligands in *bis*-bidentate fashion. The *C*2-pyrazolyl groups of each tpym ligand are oriented towards the centre of the assembly, and bind the fifth silver ion Ag(1). This complex is related to previously reported $[\mathrm{M}_4(\mu\text{-bpym})_4]^{4+}$ (bpym = 4,6-di{pyrazol-1-yl}pyrimidine, Scheme 1; M$^+$ = Cu$^+$, Ag$^+$) molecular squares,[27,36] but with an additional silver ion coordinated at the center of the assembly. Pairs of the Ag(1)-coordinated pyrazolyl groups are sandwiched between the *bis*-bidentate cores of the other bpym ligands (Fig. 6). These intramolecular $\pi...\pi$ interactions may help to stabilise the cluster assembly.

The tpym ligands bound to Ag(2) and Ag(3) both yield a sawhorse-type coordination geometry, with a near-linear N{pyrazolyl}–Ag–N{pyrazolyl} angle. The coordination sphere of Ag(3) is expanded further by weak Ag...F contacts to two symmetry-related, disordered BF$_4^-$ ions. No such secondary interactions to Ag(2) were resolved in the Fourier map, however. The other unique metal ions Ag(1) and Ag(4) have more typical flattened tetrahedral geometries. The silver ions in the cage are well-separated from each other with Ag(1)

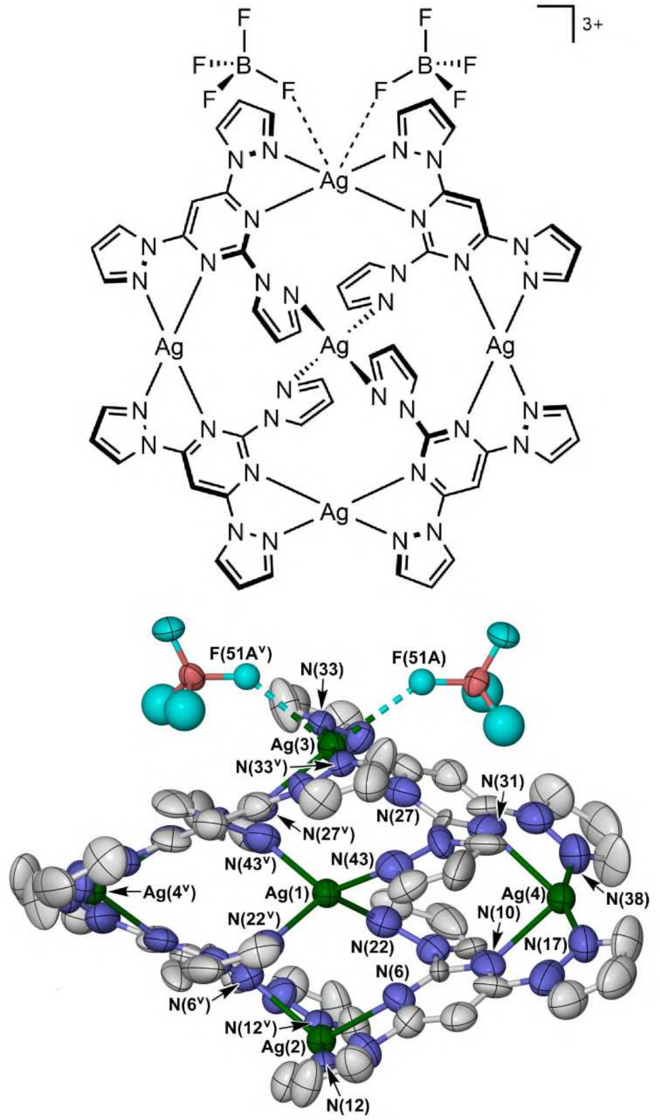

Figure 4 Schematic (top) and crystallographic view (bottom) of the pentanuclear $[\mathrm{Ag}_5(\mathrm{tpym})_4(\mathrm{BF}_4)_2]^{3+}$ assembly in **4**·2MeNO$_2$. Only one orientation of the disordered BF_4^- ion is shown. Other details as for Fig. 1. Symmetry code: (v) $1-x$, y, $^{3}/_{2}-z$. Colour code: C, white; Ag, green; B, pink; F, cyan; N, blue.

being 3.7315(16)-3.7443(16) Å from Ag(2) and Ag(3), and the other nearest-neighbour Ag...Ag distances ranging from 5.8354(9)-6.9319(11) Å.

Isostructural solvent-free salts $[\mathrm{Ag}(\mu\text{-tpt})]\mathrm{BF}_4$ (**5a**) and $[\mathrm{Ag}(\mu\text{-tpt})]\mathrm{ClO}_4$ (**5b**), obtained from acetone and 2,2,2-trifluoroethanol respectively, adopt the orthorhombic space group $Pca2_1$. Their asymmetric units contain two unique Ag/tpt moieties, which alternate within 1D coordination polymer chains along *c* (Fig. 5). Although the tpt ligands are not helically disposed the coordination polymer chains in **5a** and **5b** have helical character, the pitch of the helices being equal to the unit cell *c* dimension. The handed crystals contain either all-Λ or all-Δ helical chains (although the crystal of **5b** used in this study was a racemic twin). Each tpt ligand chelates to two silver ions in *bis*-bidentate fashion, with each silver ion also accepting a much longer secondary bonding interaction of 2.906(8)-2.964(12) Å from a third ligand pyrazolyl donor. The BF_4^- or ClO_4^- ions associate with the exterior of the helical chains, by bridging between a silver ion and a triazinyl C atom in the same $[\mathrm{Ag(tpt)}]^+$ fragment (Fig. 5). One of the two unique anions also forms a second inter-chain anion...π contact (not shown in Fig. 5; ESI†).[37] The dimensions of these secondary interactions are complicated by anion disorder, but range from C...X = 2.860(14)-3.10(3) Å (X = F or O). Those are typical values for anion...π interactions involving these residues.[38,39] The intra-chain Ag...Ag distances are 6.2119(9) and 6.5299(8) Å in **5a**, and 6.2276(15) and 6.5019(14) Å in **5b**.

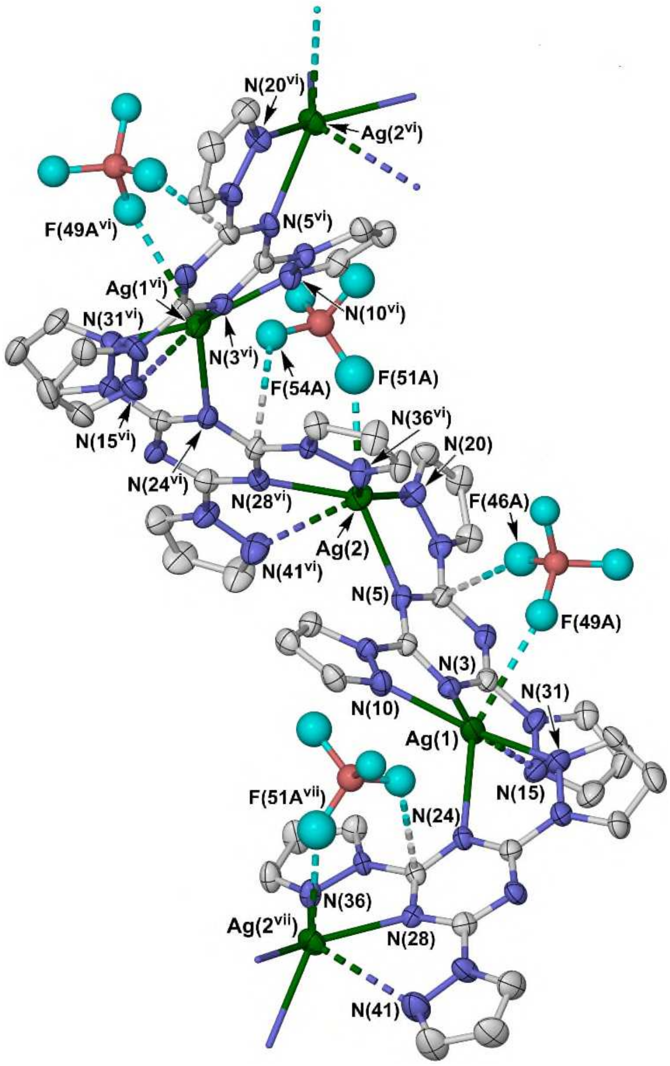

Figure 5 One turn of the helical coordination polymer chain in **5a**. Only one orientation of the disordered BF_4^- ions is shown. Other details as for Fig. 1. Symmetry codes: (vi) $1-x$, $-y$, $^{1}/_{2}+z$; (vii) $1-x$, $-y$, $-^{1}/_{2}+z$. Colour code C, white; Ag, green; B, pink; F, cyan; N, blue.

Two solvates of **5a** were also obtained. The asymmetric unit of **5a**·MeNO$_2$ (monoclinic, $P2_1$) contains two unique Ag/tpt centres, which occupy different 1D coordination polymer chains (Fig. 6). The bridging tpt ligands bind one silver ion in a tridentate [2+1] coordination mode, similar to that in the unsolvated structure, and the other in a [1+1] fashion with a longer interaction to the chelating triazinyl N donor. This gives

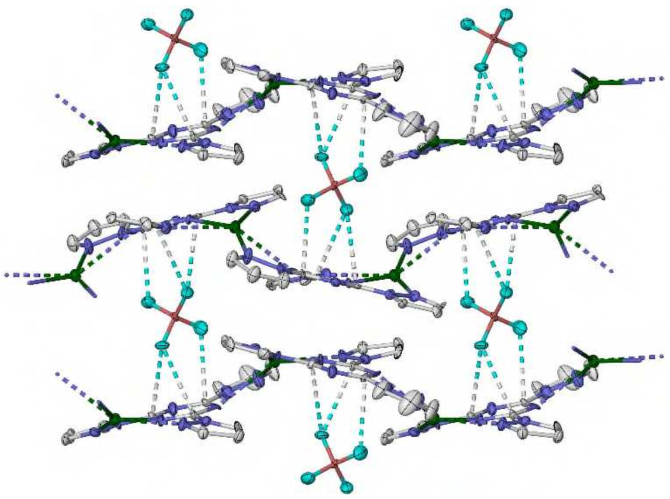

Figure 6 The coordination polymer asymmetric unit in **5a**·$MeNO_2$, showing the alternating interchain anion...π and π...π interactions. The non-interacting anion and solvent are omitted from the view, which is along the (103) crystal vector, with *b* horizontal. A fully labelled Figure of this structure is in the ESI†. Colour code C, white; Ag, green; B, pink; F, cyan; N, blue.

each Ag ion an irregular [3+2] coordination, which resembles a pentagonal pyramidal geometry. The Ag/tpt monomers assemble *via* the crystallographic 2_1 operation into non-helical zig-zag chains running parallel to *b*. One of the unique BF_4^- ions is sandwiched by strong anion...π contacts to triazinyl rings, from one polymer chain of each type (Fig. 6; C...F = 2.897(15)-3.092(14) Å).[38,39] The overall structure contains pairs of π-stacked polymer chains, which are linked into sheets in the (001) plane by alternating π...π and anion...π interactions. These sheets are separated from each other by layers containing the solvent and remaining anions.

The other solvate **5a**·MeOH (orthorhombic, *Pbca*) has a simpler structure. The tpt ligands are [2+1]-coordinated to one silver ion and bridge to another silver ion, related by the crystallographic *a* glide, in monodentate fashion through their third pyrazolyl donor (ESI†). The methanol molecule coordinates to the silver ion, and donates a hydrogen bond to the BF_4^- ion. There are no π...π or anion...π contacts in the lattice, and the coordination polymer molecules are well-separated by the hydrogen bonded anions.

Finally, [Ag(μ-bpt)]BF_4 (**6**; monoclinic, $P2_1/m$) crystallises as a simple 1D coordination polymer. The asymmetric unit contains half an empirical formula of the compound, with Ag(1) on a crystallographic inversion centre and the bpt ligand and BF_4^- ion bisected by the crystallographic mirror plane (Fig. 7). The silver ion is coordinated by two *bis*-bidentate bpt ligands in an approximately square planar geometry that is unusual in silver(I) chemistry.[40] The near-planar polymer chains run parallel to the unit cell *b* direction, and are grouped by translation into canted stacks along *a*, adjacent molecules in the stacks being coplanar and separated by 3.402(13) Å. This places the pyrazolyl rings from nearest neighbour molecules above the axial sites of the square planar Ag ion, although the shortest Ag...C distance, Ag(1)...C(9^{xxv}) = 3.041(3) Å [symmetry code: (xxv) 1+*x*, *y*, *z*] is 0.5 Å longer than expected for an alkene→Ag coordinate bond.[41] The BF_4^- ion forms a strong anion...π interaction to the bpt triazinyl ring,[37] through two short C...F contacts of 2.823(3) Å (Fig. 7).[38,39] This may contribute to the adoption of a coordination polymer structure by **4**, rather than a molecular square assembly analogous to the aforementioned Ag/bpym adducts (Scheme 1).[27,36]

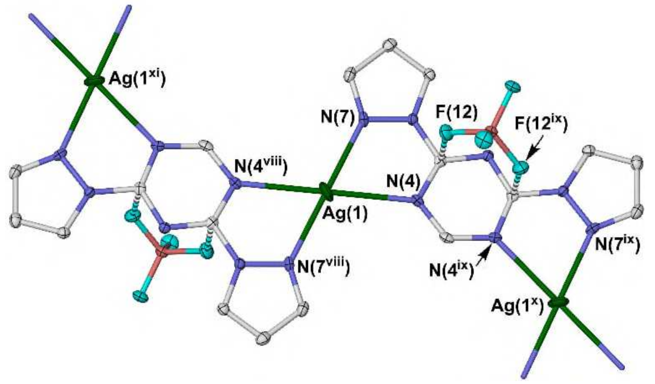

Figure 7 The coordination polymer asymmetric unit in **6**. Details as for Fig. 1. Symmetry codes: (viii) 2–*x*, 1–*y*, –*z*; (ix) *x*, $^3/_2$–*y*, *z*; (x) 2–*x*, $^1/_2$+*y*, –*z*; (xi) 2–*x*, –$^1/_2$+*y*, –*z*.

The ES mass spectra of most of these compounds from $MeNO_2$ solution are dominated by mononuclear or dinuclear fragments, reflecting the lability of silver(I) complexes in solution. However, the spectra of **4** and **5a** show a progression of $[Ag_nL_mX_{n-1}]^+$ (L = tpym or tpt; n–1 $\leq$ m $\leq$ n+1; X^- = BF_4^- and/or F^-) species up to n = 6 (ESI†). That confirms the oligomeric nature of those compounds in solution, as well as the solid state. The crystallographically observed $[Ag_5(tpym)_4]^{5+}$ cluster is evident as a very weak component in the spectrum of **4**. The apparent instability of **4** in solution is consistent with a previously reported $[Ag_4L_4]^{4+}$ molecular square supported by a chiral bpym derivative *L* ligand, which was shown conclusively to fragment in solution.[27]

Conclusion

This study has expanded the range of structures adopted by silver(I) complexes of terpy or terpy-analogue *tris*-heterocycles. While the face-to-face dimers **1** and **3** adopt a previously known structure type,[6,8-11] the aggregation of these dimers into a 1D coordination polymer in α-**2**·$MeNO_2$, through a rare $\kappa^1,\kappa^1:\mu$-pyrazolyl bridging mode,[33,34] has not been seen before. The unsupported polymer-of-helicates structure in β-**2**·$y$$MeNO_2$ is also new, being a topological isomer of the continuous spiral architecture usually found in polymeric helicates.[6,25,26] The $[Ag_5(\mu_3\text{-tpym})_4]^{5+}$ assembly in **4** is a metal-centred analogue of a family of $[M_4(\mu\text{-bpym})_4]^{4+}$ (M^+ = Cu^+, Ag^+) molecular squares.[27,36] Lastly linear, zig-zag or helical 1D coordination polymers of the 1,3,5-triazinyl ligands tpt and bpt are described, whose architectures are supported by anion... π interactions to the triazinyl ring.[38,39]

Our synthesis of bpt is also noteworthy, as the parent ligand of the 2,4-di(pyrazolyl)-1,3,5-triazine family. Derivatives of bpt substituted at the *C*6 position are well known, and have particular use as lanthanide photosensitisers[42] as well as in other aspects of coordination chemistry.[19,20,39,43] A wider investigation of the coordination chemistry of bpt is underway, and will be reported in future publications.

Experimental

The ligands tpp,[29] tpym[30] and tpt[31] were prepared by the literature procedures. Other reagents and solvents were purchased commercially and used as supplied.

Synthesis of 2,4-di(pyrazol-1-yl)-6*H*-1,3,5-triazine (bpt). Solid pyrazole (0.48 g, 7.0 mmol) was added to a suspension of NaH (60 wt% suspension in mineral oil; 0.28 g, 7.0 mmol) in dry THF (30 cm^3). After all the solid had dissolved, a suspension of 2,4-dichloro-1,3,5-triazine (0.50 g, 3.5 mmol) in THF (30 cm^3) was added to the mixture, which was then stirred at room temperature for 12 hrs. The solution was evaporated to dryness, and the residue suspended in water. The product was extracted from the aqueous layer with dichloromethane (200 cm^3), which was then dried with $MgSO_4$ and evaporated to dryness. Pure bpt was obtained as a white solid after column chromatography on silica gel (eluent: EtOAc, Rf: 0.22). Yield 0.36 g, 48%. Elemental analysis: found C, 50.7; H, 3.25; N, 45.9 %. Calcd for $C_9H_7N_7$ C, 50.7; H, 3.31; N, 46.0 %. Mp 100-101 ^oC. ESMS *m/z* 214.0 ($[Hbpt]^+$), 236.1 ($[Na(bpt)]^+$), 449.1 ($[Na(bpt)_2]^+$). ^1H NMR ($CDCl_3$) δ 6.57 (dd, 1.2 and 2.7 Hz, 2H, Pz H^4), 7.92 (s, 2H, Pz H^3), 8.69 (d, 2.7 Hz, 2H, Pz H^5), 9.07 (s, 1H, Trz H^6). ^{13}C NMR ($CDCl_3$) δ 109.8 (2C, Pz C^4), 129.6 (2C, Pz C^5), 145.2 (2C, Pz C^3), 161.7 (2C, Trz $C^{2/4}$), 168.9 (1C, Trz C^6).

Synthesis of $[Ag_2(tpp)_2(MeCN)_2][BF_4]_2$ (1). A solution of tpp (15 mg, 0.054 mmol) in MeCN (3 cm^3) was added to a solution of $AgBF_4$ (11 mg, 0.056 mmol) in MeCN (4 cm^3). Slow diffusion of diethyl ether vapour into the resultant clear solution afforded colourless crystals of **1**·2MeCN, which decompose to solvent-free **1** upon drying *in vacuo*. Yield 18 mg, 62 %. Found: C, 37.5; H, 2.80; N, 21.7 %. Calcd for $C_{32}H_{28}Ag_2B_2F_8N_{16}$: C, 37.5; H, 2.75; N, 21.8 %.

Synthesis of $[Ag_2(tpp)_2][BF_4]_2 \cdot MeNO_2$ (2·$MeNO_2$). Method as for **1**, using $MeNO_2$ as the reaction solvent. The product formed as a mixture of two morphologies, which proved to be the α and β solvatomorphs described in the text. Bulk samples of the material analyse with a formulation similar to α-**2**·$MeNO_2$, which is also the major morphology present in the crystallisation vials. Yield 23 mg, 83 %. Found: C, 34.5; H, 2.42; N, 20.7 %. Calcd for $C_{28}H_{22}Ag_2B_2F_8N_{14} \cdot CH_3NO_2$ C, 34.7; H, 2.51; N, 20.9 %. ESMS *m/z* 384.01 (100, $[Ag(tpp)]^+$), 661.11 (83, $[Ag(tpp)_2]^+$), 857.02 (24, $[Ag_2(tpp)_2(BF_4)]^+$), 1328.03 (3, $[Ag_3(tpp)_3(BF_4)_2]^+$).

Synthesis of $[Ag_2(tpym)_2(MeCN)_2][BF_4]_2$ (3). Method as for **1**, using tpym (21 mg, 0.075 mmol) and with the other quantities adjusted appropriately. The compound forms colourless needles from MeCN/Et_2O. Yield 34 mg, 87 %. Found: C, 34.7; H, 2.32; N, 24.0 %. Calcd for $C_{30}H_{26}Ag_2B_2F_8N_{18}$: C, 35.1; H, 2.55; N, 24.5 %.

Synthesis of $[Ag_5(tpym)_4][BF_4]_5 \cdot 2MeNO_2$ (4·2$MeNO_2$). A solution of tpym (26 mg, 0.09 mmol) in $MeNO_2$ (4 cm^3) was added to a solution of $AgBF_4$ (22.7 mg, 0.117 mmol) in $MeNO_2$ (6 cm^3). Slow diffusion of diethyl ether vapour into the resultant clear solution afforded colourless crystals of **4**·2$MeNO_2$, which decompose to solvent-free **4** upon drying *in vacuo*. Yield 34 mg, 71 %. Found: C, 29.8; H, 1.96; N, 21.3 %. Calcd for $C_{52}H_{40}Ag_5B_5F_{20}N_{32}$: C, 29.9; H, 1.93; N, 21.5; %. ESMS: *m/z* 663.24 (18, $[Ag(tpym)_2]^+$), 772.01 (35, $[Ag_2(tpym)_2]^+$), 791.01 (100, $[Ag_2(tpym)_2F]^+$), 859.01 (82, $[Ag_2(tpym)_2BF_4]^+$), 898.01 (5, $[Ag_3(tpym)_2F]^+$), 917.01 (5, $[Ag_3(tpym)_2F_2]^+$), 984.91 (21, $[Ag_3(tpym)_2(BF_4)F]^+$), 1053.91 (5, $[Ag_3(tpym)_2(BF_4)_2]^+$), 1330.92 (2, $[Ag_3(tpym)_3(BF_4)_2]^+$), 1526.92 (7, $[Ag_4(tpym)_3(BF_4)_3]^+$), 1720.94 (2, $[Ag_5(tpym)_3(BF_4)_4]^+$), 1998.94 (2, $[Ag_5(tpym)_4(BF_4)_4]^+$), 2194.95 (4, $[Ag_6(tpym)_4(BF_4)_5]^+$).

Synthesis of $[Ag(tpt)]BF_4$ (5a) A solution of tpt (20 mg, 0.071 mmol) in nitromethane (2.5 cm^3) was added to a hot solution of $AgBF_4$ (14 mg, 0.071 mmol) in nitromethane (8 cm^3). Diethyl ether was added to the resultant transparent solution, leading to the formation of a white precipitate which was collected and dried. Yield 33 mg, 98 %. Found: C, 30.6; H, 2.10; N, 26.7 %. Calcd for $C_{12}H_9AgBF_4N_9$: C, 30.4; H, 1.91; N, 26.6 %. ESMS *m/z* 386.00 (47, $[Ag(tpt)]^+$), 667.14 ($[Ag(tpt)_2]^+$), 773.01 (10, $[Ag_2(tpt)_2]^+$), 793.01 (67, $[Ag_2(tpt)_2F]^+$), 861.01 (100, $[Ag_2(tpt)_2BF_4]^+$), 986.91 (10, $[Ag_3(tpt)_2(BF_4)F]^+$), 1054.92 (4, $[Ag_3(tpt)_2(BF_4)_2]^+$), 1138.11 (7, $[Ag_2(tpt)_3BF_4]^+$), 1334.02 (76, $[Ag_3(tpt)_3(BF_4)_2]^+$), 1461.87 (13, $[Ag_4(tpt)_3(BF_4)_2F]^+$), 1529.93 (6, $[Ag_4(tpt)_3(BF_4)_3]^+$), 1809.03 (18, $[Ag_4(tpt)_4(BF_4)_3]^+$), 2002.94 (5, $[Ag_5(tpt)_4(BF_4)_4]^+$), 2088.12 (3, $[Ag_4(tpt)_5(BF_4)_3]^+$), 2283.04 (6, $[Ag_5(tpt)_5(BF_4)_4]^+$), 2478.13 (2, $[Ag_6(tpt)_5(BF_4)_5]^+$), 2758.03 (2, $[Ag_6(tpt)_6(BF_4)_5]^+$).

Synthesis of $[Ag(tpt)]ClO_4$ (5b) Method as for **5a**, using $AgClO_4$ (15 mg, 0.072 mmol) and acetone as the solvent. The product was obtained as a white precipitate. Yield 23 mg, 68 %. Found: C, 29.8; H, 1.76; N, 25.9 %. Calcd for $C_{12}H_9AgClN_9O_4$: C, 29.6; H, 1.86; N, 25.9 %.

Synthesis of $[Ag(bpt)]BF_4$ (6). Method as for **1**, using bpt (15 mg, 0.071 mmol) and $MeNO_2$ as the reaction solvent. The product is a white polycrystalline solid. Yield: 16 mg, 57 %. Found: C, 26.4; H, 1.67; N, 23.9 %. Calcd for $C_9H_7AgBF_4N_7$ C, 26.5; H, 1.73; N, 24.0 %. ESMS *m/z* 329.98 (100, $[Ag(bpt)]^+$), 533.05 (35, $[Ag(bpt)_2]^+$).

Single crystal X-ray structure determinations

Single crystals of the compounds were grown by slow vapour diffusion of diethyl ether into solutions of the compounds. Nitromethane was used as the crystallisation solvent, except in the following cases: **1**·2MeCN and **3** (acetonitrile); **5a** (acetone); **5b** (2,2,2-trifluoroethanol); and **5a**·2MeOH (methanol). The diffraction data for **4**·2$MeNO_2$ were recorded at station I19 of the Diamond synchrotron (λ = 0.6998 Å). All the other crystallographic data were measured with an Agilent Supernova dual-source diffractometer, using monochromated Cu-K_α (λ = 1.5418 Å) or Mo-K_α (λ = 0.71073 Å) radiation. The diffractometer was fitted with an Oxford Cryostream low-temperature device. The structures were all solved by direct methods (*SHELXS97*[44]), and developed by full least-squares refinement on F^2 (*SHELXL97*[44]). Crystallographic figures were prepared using *XSEED*.[45]

X-ray structure refinements

Unless otherwise stated, the following refinement procedures were followed. Crystallographically ordered non-H atoms in the structures were refined anisotropically, while H atoms were placed in calculated positions and refined using a riding model. Disordered anions were modelled using refined distance and angle restraints, while disordered solvent molecules were treated with fixed restraints.

No disorder is present in the refinement of the bpt ligand. All H atoms in this light-atom structure were located in the Fourier map and refined, with U_{iso} constrained to 1.2xU_{eq} of the corresponding C atom.

The asymmetric unit of $[Ag_2(tpp)_2(MeCN)_2][BF_4]_2{\cdot}2MeCN$ (**1**·2MeCN) contains half a dimeric molecule spanning a crystallographic inversion centre, and one unique BF_4^- and acetonitrile molecule. The BF_4^- ion is disordered about three equally populated sites, while the solvent molecule was also refined over two orientations, whose occupancy ratio refined to 0.64:0.36.

The asymmetric unit of α-$[Ag_2(tpp)_2][BF_4]_2{\cdot}MeNO_2$ (α-**2**·$MeNO_2$) contains one dimeric complex moiety; two BF_4^- ions and one nitromethane molecule all lying on general crystallographic sites. The nitromethane molecule is disordered over two sites with refined occupancies of 0.80 and 0.20, which refined successfully without restraints.

The asymmetric unit of β-$[Ag_2(tpp)_2][BF_4]_2{\cdot}y MeNO_2$ (β-**2**·$y MeNO_2$) contains two dimeric complex cations, four BF_4^- ions and one partial nitromethane molecule. Three of the four unique uncoordinated pyrazolyl groups are disordered, over two orientations. In one case, this may be connected to the

Table 1 Experimental details for the crystal structure determinations in this work.

	bpt	**1**·2MeCN	α-**2**·$MeNO_2$	β-**2**·$y MeNO_2$ ($y \approx 0.3$)	**3**	**4**·$2MeNO_2$
Molecular formula	$C_9H_7N_7$	$C_{36}H_{34}Ag_2B_2F_8N_{18}$	$C_{29}H_{25}Ag_2B_2F_8N_{15}O_2$	$C_{28.31}H_{22.92}Ag_2B_2F_8N_{14.31}O_{0.61}$	$C_{30}H_{26}Ag_2B_2F_8N_{18}$	$C_{54}H_{46}Ag_5B_5F_{20}N_{34}O_4$
M_r	213.22	1108.17	1005.00	962.57	1028.05	2208.65
Crystal class	monoclinic	monoclinic	triclinic	monoclinic	monoclinic	monoclinic
Space group	$P2_1/n$	$P2_1/c$	$P\overline{1}$	$P2_1/c$	$P2_1$	$C2/c$
a (Å)	14.3972(8)	12.0945(3)	12.1548(7)	25.2916(6)	11.3714(3)	29.8766(6)
b (Å)	4.1060(2)	6.8744(2)	12.6789(8)	11.6686(3)	6.8555(2)	10.9444(2)
c (Å)	16.4295(11)	26.4084(6)	13.5860(8)	23.1019(5)	23.7996(6)	25.5649(8)
α (°)	–	–	66.821(6)	–	–	–
β (°)	103.275(7)	93.926(2)	65.231(5)	91.719(2)	90.420(2)	115.208(2)
γ (°)	–	–	72.775(5)	–	–	–
V (Å^3)	945.28(9)	2190.51(10)	1725.93(18)	6814.7(3)	1855.29(9)	7563.2(3)
Z	4	2	2	4	2	4
T(K)	120(2)	120(2)	120(2)	120(2)	120(2)	100(2)
μ (mm^{-1})	0.857[a]	7.929[a]	1.235[b]	10.059[a]	9.303[a]	1.391[c]
Measured reflections	3204	8334	18262	29229	8140	15662
Independent reflections	1814	4291	8207	13111	5174	5480
R_{int}	0.030	0.031	0.028	0.039	0.027	0.042
R_1, $I > 2\sigma(I)$[d]	0.043	0.057	0.036	0.054	0.051	0.087
wR_2, all data[e]	0.116	0.162	0.075	0.151	0.135	0.270
Flack parameter	–	–	–	–	0.045(13)	–
	5a	**5b**	**5a**·$MeNO_2$	**5a**·MeOH	**6**	
Molecular formula	$C_{12}H_9AgBF_4N_9$	$C_{12}H_9AgClN_9O_4$	$C_{13}H_{12}AgBF_4N_{10}O_2$	$C_{13}H_{13}AgBF_4N_9O$	$C_9H_7AgBF_4N_7$	
M_r	473.96	486.60	535.01	506.00	407.90	
Crystal class	orthorhombic	orthorhombic	monoclinic	orthorhombic	monoclinic	
Space group	$Pca2_1$	$Pca2_1$	$P2_1$	$Pbca$	$P2_1/m$	
a (Å)	17.9041(8)	18.3941(9)	10.8501(6)	15.4505(4)	5.6623(1)	
b (Å)	10.1194(3)	10.1003(3)	12.4336(6)	13.9523(4)	14.2076(3)	
c (Å)	18.2383(6)	18.0884(7)	14.5101(9)	16.3341(4)	7.7351(2)	
α (°)	–	–	–	–	–	
β (°)	–	–	108.445(7)	–	91.837(2)	
γ (°)	–	–	–	–	–	
V (Å^3)	3304.4(2)	3360.6(2)	1856.94(18)	3521.14(16)	621.95(2)	
Z	8	8	2	8	2	
T(K)	120(2)	120(2)	120(2)	120(2)	120(2)	
μ (mm^{-1})	10.380[a]	11.498[a]	9.424[a]	9.831[a]	13.589[a]	
Measured reflections	13057	8711	8889	20146	2286	
Independent reflections	6138	4890	5181	3515	1240	
R_{int}	0.054	0.044	0.052	0.034	0.030	
R_1, $I > 2\sigma(I)$[d]	0.047	0.066	0.086	0.027	0.038	
wR_2, all data[e]	0.123	0.184	0.224	0.066	0.106	
Flack parameter	–0.003(10)	0.522(17)	0.150(17)	–	–	

[a]Collected with Cu-$K\alpha$ radiation. [b]Collected with Mo-$K\alpha$ radiation. [c]Collected with synchrotron radiation. [d]$R = \Sigma[|F_o| - |F_c|] / \Sigma|F_o|$. [e]$wR = [\Sigma w(F_o^2 - F_c^2) / \Sigma wF_o^4]^{1/2}$

partial occupancy of the nitromethane molecule, which occupies a neighbouring site in the lattice and refined to an occupancy of 0.6. No restraints were applied to the disordered residues in the model, except for an anti-bumping restraint between H atoms on different, disordered pyrazole groups.

Although its unit cell parameters closely resemble **1**·2MeCN, the asymmetric unit of $[Ag_2(tpym)_2(MeCN)_2][BF_4]_2$ (**3**) lacks a crystallographic inversion centre, and contains a full molecule of the complex salt. One of the two unique BF_4^- ions is disordered over two sites, whose occupancies refined to 0.62 and 0.38. The *N*3 and *C*5 pyrimidinyl ring atom sites in both ligands [N(5)/C(7) and N(26)/C(28) in the model] were clearly distinguishable from their displacement parameters.

The asymmetric unit of $[Ag_5(tpym)_4][BF_4]_5 \cdot 2MeNO_2$ (**4**·$2MeNO_2$) contains half a complex molecule with Ag(1), Ag(2) and Ag(3) all lying on the same crystallographic C_2 axis; and, one BF_4^- ion that is disordered over three equally occupied sites by rotation around one B–F bond. The remaining unit cell contents, including the three extra BF_4^- ions expected for charge balance, are contained in large rectangular channels running parallel to the unit cell *b* axis. These have a volume per unit cell of 1972.4 Å^3, or 26.1 % of the total cell volume. A *SQUEEZE* analysis[35] showed these contain 745 electrons per unit cell, or 186 electrons per formula unit. That corresponds perfectly to three BF_4^- ions (41 electrons each) + two nitromethane molecules (32 electrons each), which were included in the molecular formula and density calculation. The *SQUEEZE*d dataset was used in the final least squares refinement cycles.

The isostructural crystals $[Ag(tpt)]BF_4$ (**5a**) and $[Ag(tpt)]ClO_4$ (**5b**) contain two formula units of the coordination polymer in their asymmetric units. While the crystal of the BF_4^- salt was optically pure in the handed space group $Pca2_1$, the ClO_4^- salt was refined as a racemic twin. Both unique anions are disordered in each structure, over two or three orientations. All non-H atoms, plus the half-occupied partial ClO_4^- ions in **3b**, were refined anisotropically.

The asymmetric unit of $[Ag(tpt)]BF_4 \cdot MeNO_2$ (**5a**·$MeNO_2$) contains two formula units, comprising monomer units from two different polymer chains of the silver complex. The crystal used was a mild racemic twin [Flack parameter = 0.150(17)], which might indicate the presence of a minor non-merohedral twin domain in the dataset. No positional disorder is present in the model, but DELU restraints were applied to address non-positive-definite errors in atoms N(6) and C(17).

No disorder is present in $[Ag(tpt)(MeOH)]BF_4$ (**5a**·MeOH), and no restraints were applied to the refinement. The methanol O-bound H atom was located in the Fourier map and allowed to refine, with U_{iso} constrained to U_{eq} of the corresponding O atom. The other H atoms in the model were treated as above.

The asymmetric unit of $[Ag(bpt)]BF_4$ (**6**) also contains half an empirical formula unit of the compound, with Ag(1) lying on a crystallographic inversion centre; N(2) and C(5) on the mirror plane *x*, ¾, *y*; and the B atom and two F atoms from the half-anion on the same mirror plane. There is no disorder in this structure.

Other measurements

Elemental microanalyses were performed by the microanalytical services at the University of Leeds School of Chemistry, or the London Metropolitan University School of Human Sciences. Electrospray mass spectra were recorded on a Bruker MicroTOF-q instrument, from $CHCl_3$ solution (organic compounds) or CH_3NO_2 solution (metal complexes). NMR spectra employed a Bruker DPX300 spectrometer operating at 300.1 MHz (^{1}H) or 75.5 MHz (^{13}C). X-ray powder diffraction patterns were measured using a Bruker D2 Phaser diffractometer.

Conflicts of interest

There are no conflicts to declare.

Acknowledgements

This work was funded by the Leverhulme Trust (RPG-2015-095). We thank Diamond Light Source for access to beamline I19 (MT10334) that contributed to the results presented here.

Notes and references

1 S. bin Silong, J. D. Kildea, W. Patalinghug, B. W. Skelton and A. H. White, *Aust. J. Chem.*, 1994, **47**, 1545.
2 E. C. Constable, A. J. Edwards, G. R. Haire, M. J. Hannon and P. R. Raithby, *Polyhedron*, 1998, **17**, 243.
3 L. Hou, D. Li, Y. G. Yin, T. Wu and S. W. Ng, *Acta Cryst. Sect. E: Struct. Rep. Online*, 2004, **60**, m1106.
4 G. Baum, E. C. Constable, D. Fenske, C. E. Housecroft and T. Kulke, *Chem. Commun.*, 1998, 2659; G. Baum, E. C. Constable, D. Fenske, C. E. Housecroft, T. Kulke, M. Neuburger and M. Zehnder, *J. Chem. Soc.*, *Dalton Trans*., 2000, 945.
5 J. E. Aguado, M C. Gimeno, P. G. Jones and A. Laguna, *Can. J. Chem.*, 2009, **87**, 341.
6 M. J. Hannon, C. L. Painting, E. A. Plummer, L. J. Childs and N. W. Alcock, *Chem. Eur. J.*, 2002, **8**, 2226.
7 S. Sharma, G. J. E. Davidson and S. J. Loeb, *Chem. Commun.*, 2008, 582; G. Golubkov, H. Weissman, E. Shirman, S. G. Wolf, I. Pinkas and B. Rybtchinski, *Angew. Chem., Int. Ed.*, 2009, **48**, 926.
8 L. Hou, D. Lia and S. W. Ng, *Acta Cryst. Sect. E: Struct. Rep. Online*, 2005, **61**, m404.
9 R. Zibaseresht and R. M. Hartshorn, *Dalton Trans.*, 2005, 3898.
10 C.-J. Chen, F.-N. Liu, A.-J. Zhang, L.-W. Zhang and X. Liu, *Acta Cryst. Sect. E: Struct. Rep. Online*, 2009, **65**, m1674.
11 R.-L. Chen, X.-Y. Chen, S.-R. Zheng, J. Fan and W.-G. Zhang, *Cryst. Growth Des.*, 2013, **13**, 4428.
12 Y. Ma, B. Liu and C. Xue, *Acta Cryst. Sect. E: Struct. Rep. Online*, 2010, **66**, m1117.
13 J. Heine, H. Westemeier and S. Dehnen, *Z. Anorg. Allg. Chem.*, 2010, **636**, 996.
14 G. A. Bowmaker, Effendy, P. C. Junk, B. W. Skeleton and A. H. White, *Z. Naturforsch., Teil B: Chem. Sci.*, 2004, **59**, 1277.
15 Z. Ma, Y. Xing, M. Yang, M. Hua, B. Liu, M. Fátima C. Guedes da Silva and A. J. L. Pombeiro, *Inorg, Chim, Acta*, 2009, **362**, 2921.
16 Paul K.-K. Ho, S.-M. Peng, K.-Y. Wong and C.-M. Che, *J. Chem. Soc., Dalton Trans.*, 1996, 1829; Y. Cui and C. He, *J. Am. Chem. Soc.*, 2003, **125**, 16202; M. A. Fik, A. Gorczyński, M. Kubicki, Z. Hnatejko, A. Fedoruk-Wyszomirska, E. Wyszko, M.

Giel-Pietraszuk and V. Patroniak, *Eur. J. Med. Chem.*, 2014, **86**, 456.

17 L. Hou and D. Li, *Inorg. Chem. Commun.*, 2005, **8**, 128.

18 M. Gil-Moles, M. C. Gimeno, J. M. Lopez-de-Luzuriaga, M. Monge, M. E. Olmos and D. Pascual, *Inorg. Chem.*, 2017, **56**, 9281.

19 C. Yang, O. Elbjeirami, C. S. P. Gamage, H. V. R. Dias and M. A. Omary, *Chem. Commun.*, 2011, **47**, 7434; M. P. Carranza, B. R. Manzano, F. A. Jalón, A. M. Rodríguez, L. Santos and M. Moreno, *New J. Chem.*, 2013, **37**, 3183.

20 M. P. Carranza, B. R. Manzano, F. A. Jalón, A. M. Rodríguez, L. Santos and M. Moreno, *Inorg. Chem.*, 2010, **49**, 3828.

21 N. K. Solanki, A. E. H. Wheatley, S. Radojevic, M. McPartlin and M. A. Halcrow, *J. Chem. Soc*., *Dalton Trans*., 1999, 521; M. Loï, M. W. Hosseini, A. Jouaiti, A. De Cian and J. Fischer, *Eur. J. Inorg. Chem.*, 1999, 1981; O. Atakol, H. Fuess, R. Kurtaran, A. Akay, C. Arici, Ü. Ergun and K. C. Emregül, *J. Therm. Anal. Calorim.*, 2007, **90**, 517.

22 C. Provent, S. Hewage, G. Brand, G. Bernardinelli, L. J. Charbonnière and A. F. Williams, *Angew. Chem., Int. Ed.*, 1997, **36**, 1287.

23 G. M. Borrajo-Calleja, E. de Julián, E. Bayón, J. Díez, E. Lastra, I. Merino and M. P. Gamasa, *Inorg. Chem.*, 2016, **55**, 8794.

24 H. Oshio, M. Yamamoto and T. Ito, *J. Chem. Soc*., *Dalton Trans*., 1999, 2641.

25 Y. Zhou, W. Chen and D. Wang, *Dalton Trans.*, 2008, 1444.

26 H.-W. Kuai, X.-C. Cheng, D.-H.Li, T. Hu and X.-H. Zhu, *J. Solid State Chem.*, 2015, **228**, 65; C.-H. Dai and F.-L. Mao, *Z. Naturforsch. Teil B Chem. Sci.*, 2015, **70**, 851.

27 M. C. Carrión, I. M. Ortiz, F. A. Jalón, B. R. Manzano, A. M. Rodríguez and J. Elguero, *Cryst. Growth Des.*, 2011, **11**, 1766.

28 M. A. Halcrow, *Coord. Chem. Rev.*, 2009, **253**, 2493; M. A. Halcrow, *New J. Chem.*, 2014, **38**, 1868.

29 L. J. Kershaw Cook, R. Mohammed, G. Sherborne, T. D. Roberts, S. Alvarez and M. A. Halcrow, *Coord. Chem. Rev.*, 2015, **289–290**, 2.

30 A. Gelling, D. R. Noble, K. G. Orrell, A. G. Osborne and V. Sik, *J. Chem. Soc*., *Dalton Trans*., 1996, 3065.

31 V. Milata, R. M. Claramunt, P. Cabildo, M. D. Santa María, P. Cornago, L. Infantes, F. H. Cano and J. Elguero, *Heterocycles*, 2001, **55**, 905.

32 A. W. Addison, T. N. Rao, J. Reedijk, J. van Rijn and G. C. Verschoor, *J. Chem. Soc., Dalton Trans.*, 1984, 1349.

33 See *eg* C. Mealli, C. S. Arcus, J. L. Wilkinson, T. J. Marks and J. A. Ibers, *J. Am. Chem. Soc.*, 1976, **98**, 711; O. Kuhl, J. Sieler and E. Hey-Hawkins, *Main Group Met. Chem.*, 2001, **24**, 39; S. Bieller, F. Zhang, M. Bolte, J. W. Bats, H.-W. Lerner and M. Wagner, *Organometallics*, 2004, **23**, 2107; A. H. Ilkhechi, J. M. Mercero, I. Silanes, M. Bolte, M. Scheibitz, H.-W. Lerner, J. M. Ugalde and M. Wagner, *J. Am. Chem. Soc.*, 2005, **127**, 10656; M. H. Chisholm, J. C. Gallucci and G. Yaman, *Inorg. Chem.*, 2007, **46**, 8676; K. Ruth, S. Tullmann, H. Vitze, M. Bolte, H.-W. Lerner, M. C. Holthause and M. Wagner, *Chem. Eur. J.*, 2008, **14**, 6754; D. Sambade and G. Parkin, *Polyhedron*, 2017, **125**, 219.

34 X. Liu, J. A. McAllister, M. P. de Miranda, E. J. L. McInnes, C. A. Kilner and M. A. Halcrow, *Chem. Eur. J.*, 2004, **10**, 1827; I. Bassanetti, C. Atzeri, D. A. Tinonin and L. Marchio, *Cryst. Growth Des.,* 2016, **16**, 3543; I. Bassanetti, M. Mattarozzi, M. Delferro, T. J. Marks and L. Marchio, *Eur. J. Inorg. Chem.*, 2016, 2626.

35 A. L. Spek, *Acta Cryst. Sect. C.: Struct. Chem.*, 2015, **71**, 9.

36 B. R. Manzano, F. A. Jalón, I. M. Ortiz, M. L. Soriano, F. Gómez de la Torre, J. Elguero, M, A. Maestro, K. Mereiter and T. D. W. Claridge, *Inorg. Chem.*, 2008, **47**, 413; I. M. Ortiz, M. L. Soriano, M. P. Carranza, F. A. Jalón, J. W. Steed, K. Mereiter, A. M. Rodríguez, D. Quiñonero, P. M. Deyà and B. R. Manzano, *Inorg. Chem.*, 2010, **49**, 8828.

37 A. Frontera, P. Gamez, M. Mascal, T. J. Mooibroek and J. Reedijk, *Angew. Chem., Int. Ed.*, 2011, **50**, 9564; H. T. Chifotides and K. R. Dunbar, *Acc. Chem. Res.*, 2013, **46**, 894; A. Frontera, *Coord. Chem. Rev.*, 2013, **257**, 1716; A. Bauzá, T. J. Mooibroek and A. Frontera, *CrystEngComm*, 2016, **18**, 10; M. Giese, M. Albrecht and K. Rissanen, *Chem. Commun.,* 2016, **52**, 1778.

38 See *eg* S. Demeshko, S. Dechert and F. Meyer, *J. Am. Chem. Soc.*, 2004, **126**, 4508; H. Casellas, C. Massera, F. Buda, P. Gamez and J. Reedijk, *New J. Chem.*, 2006, **30**, 1561 ; L. A. Barrios, G. Aromí, A. Frontera, D. Quiñonero, P. M. Deyà, P. Gamez, O. Roubeau, E. J. Shotton and S. J. Teat, *Inorg. Chem.*, 2008, **47**, 5873; D.-X. Wang and M.-X. Wang, *J. Am. Chem. Soc.*, 2013, **135**, 892; D. A. Safin, A. Pialat, A. A. Leitch, N. A. Tumanov, I. Korobkov, Y. Filinchuk, J. L. Brusso and M. Murugesu, *Chem. Commun.*, 2015, **51**, 9547.

39 D. Quiñonero, P. M. Deyà, M. P. Carranza, A. M. Rodríguez, F. A. Jalón and B. R. Manzano, *Dalton Trans.*, 2010, **39**, 794.

40 A. G. Young and L. R. Hanton, *Coord. Chem. Rev.*, 2008, **252**, 1346.

41 J. Burgess and P. J. Steel, *Coord. Chem. Rev.*, 2011, **255**, 2094.

42 See *eg* L.-M. Fu, X.-F. Wen, X.-C. Ai, Y. Sun, Y.-S. Wu, J.-P. Zhang and Y. Wang, *Angew. Chem., Int. Ed.*, 2005, **44**, 747; M. I. J. Stich, M. Schaeferling and O. S. Wolfbeis, *Adv. Mater.*, 2009, **21**, 2216; G.-L. Law, K.-L. Wong, H.-L. Tam, K.-W. Cheah and W.-T. Wong, *Inorg. Chem.*, 2009, **48**, 10492; G. Shao, R. Han, Y. Ma, M. Tang, F. Xue, Y. Sha and Y. Wang, *Chem. Eur. J.*, 2010, **16**, 8647; W. Deng, D. Jin, K. Drozdowicz-Tomsia, J. Yuan, J. Wu and E. M. Goldys, *Adv. Mater.*, 2011, **23**, 4649; W.-S. Lo, J. Zhang, W.-T. Wong and G.-L. Law, *Inorg. Chem.*, 2015, **54**, 3725; M. Tang, Y. Huang, Y. Wang and L. Fu, *Dalton Trans.*, 2015, **44**, 7449; S. K. Behzad, M. M. Amini, M. Ghanbari, M. Janghouri, P. Anzenbacher jr. and S. W. Ng*, Eur. J. Inorg. Chem.*, 2017, 3644.

43 See *eg* A. Gelling, K. G. Orrell, A. G. Osborne and V. Sik, *J. Chem. Soc., Dalton Trans.*, 1996, 3371; M. C. Carrion, A. Guerrero, F. A. Jalón, B. R. Manzano, A. de la Hoz, R. M. Claramunt, V. Milata and J. Elguero, *Inorg. Chem.*, 2003, **42**, 885; A. Guerrero, F. A. Jalón, B. R. Manzano, A. Rodríguez, R. M. Claramunt, P. Cornago, V. Milata and J. Elguero, *Eur. J. Inorg. Chem.* 2004, 549; H.-P. Zhou, X.-P. Gan, X.-L. Li, Z.-D. Liu, W.-Q. Geng, F.-X. Zhou, W.-Z. Ke, P. Wang, L. Kong, F.-Y. Hao, J.-Y. Wu and Y.-P. Tian*, Cryst. Growth Des.*, 2010, **10**, 1767; C. Chen, Q. Sun, D.-X. Ren, R. Zhang, F.-Y. Bai, Y.-H. Xing and Z. Shi, *CrystEngComm*, 2013, **15**, 5561; Z. N. Wang, X. Wang, S. Y. Wei, J. X. Wang, F.-Y. Bai, Y.-H. Xing and L. X. Sun, *New J. Chem.*, 2015, **39**, 4168; I. Capel Berdiell, R. Kulmaczewski and M. A. Halcrow, *Inorg. Chem.*, 2017, **56**, 8817.

44 G. M. Sheldrick, *Acta Cryst. Sect. C.: Struct. Chem.*, 2015, **71**, 3.

45 L. J. Barbour, *J. Supramol. Chem.*, 2001, **1**, 189.